

1

2

3

4 Regulation of gene transcription by thyroid hormone receptor β agonists in clinical
5 development for the treatment of non-alcoholic steatohepatitis (NASH)

6

7

8 Xuan G. Luong^{1*}, Sarah K. Stevens¹, Andreas Jekle¹, Tse-I Lin², Kusum Gupta¹, Dinah Misner¹, Sushmita
9 Chanda¹, Sucheta Mukherjee¹, Caroline Williams¹, Antitsa Stoycheva¹, Lawrence M. Blatt¹, Leonid N.
10 Beigelman¹, Julian A. Symons¹, Pierre Raboisson², David McGowan², Koen Vandyck², and Jerome Deval^{1*}

11 ¹Aligos Therapeutics, Inc., South San Francisco, CA, United States of America; ²Aligos Belgium BV,
12 Leuven, Belgium

13

14 * Corresponding authors

15 E-mail: xluong@aligos.com (XGL), jdeval@aligos.com (JD)

16 Abstract

17 Thyroid hormones are important modulators of metabolic activity in mammals and alter cholesterol
18 and fatty acid levels through activation of the nuclear thyroid hormone receptor (THR). Currently, there are
19 several THR β agonists in clinical trials for the treatment of non-alcoholic steatohepatitis (NASH) that have
20 demonstrated the potential to reduce liver fat and restore liver function. In this study, we tested three THR β -
21 agonism-based NASH treatment candidates, GC-1 (sobetirome), MGL-3196 (resmetirom), and VK2809,
22 and compared their selectivity for THR β and their ability to modulate the expression of genes specific to
23 cholesterol and fatty acid biosynthesis and metabolism *in vitro* using human hepatic cells and *in vivo* using
24 a rat model. Treatment with GC-1 upregulated the transcription of *CPT1A* in the human hepatocyte-derived
25 Huh-7 cell line with a dose-response comparable to that of the native THR ligand, triiodothyronine (T3).
26 VK2809A (active parent of VK2809), MGL-3196, and VK2809 were approximately 30-fold, 1,000-fold, and
27 2,000-fold less potent than T3, respectively. Additionally, these relative potencies were confirmed by
28 quantification of other direct gene targets of THR, namely, *ANGPTL4* and *DIO1*. In primary human
29 hepatocytes, potencies were conserved for every compound except for VK2809, which showed significantly
30 increased potency that was comparable to that of its active counterpart, VK2809A. In high-fat diet fed rats,
31 a single dose of T3 significantly reduced total cholesterol levels and concurrently increased liver *Dio1* and
32 *Me1* RNA expression. MGL-3196 treatment resulted in concentration-dependent decreases in total and
33 low-density lipoprotein cholesterol with corresponding increases in liver gene expression, but the compound
34 was significantly less potent than T3. In conclusion, we have implemented a strategy to rank the efficacy of
35 THR β agonists by quantifying changes in the transcription of genes that lead to metabolic alterations, an
36 effect that is directly downstream of THR binding and activation.

37

38 Introduction

39 Non-alcoholic fatty liver disease (NAFLD), characterized by $\geq 5\%$ hepatic fat accumulation,
40 encompasses a heterogenous series of disorders ranging from liver steatosis to more severe non-alcoholic
41 steatohepatitis (NASH), which may include inflammatory cell infiltration, hepatocyte ballooning, and fibrosis
42 [1, 2]. In its most severe form, NASH can progress to liver cirrhosis and hepatocellular carcinoma. Although
43 estimates vary among studies, the worldwide prevalence of NAFLD could be as high as 25% [3]. The
44 American Liver Foundation estimated that NAFLD is the most common cause of chronic liver disease in
45 the United States, affecting between 80 and 100 million individuals. Twenty percent of these patients
46 develop NASH, representing approximately 5% of total adults. Common NAFLD/NASH comorbidities
47 include obesity, type II diabetes, hyperlipidemia, hypertension, and metabolic syndrome [3]. In the absence
48 of any approved treatment, the medical burden and healthcare costs associated with NASH are immense.

49 Research on the medical treatment of NASH consists of modulating either sugar or fat metabolism
50 or targeting one of the downstream pathways associated with liver inflammation and fibrosis [4, 5]. The
51 largest class of molecular targets for hormone-based NASH therapies is nuclear receptors [6, 7]. There are
52 currently several small molecule drug candidates at various stages of clinical trial evaluation. These include
53 the farnesoid X receptor agonists, obeticholic acid and cilofexor, as well as the peroxisome proliferator-
54 activated receptor agonists, lanifibranor, pioglitazone, elafibranor, and seladelpar. Thyroid hormone
55 receptors (THR α s) represent the third class of nuclear receptors targeted for potential NASH therapy [8, 9].
56 Endogenous thyroid hormones (THs), T $_4$ and T $_3$ (Fig 1A), are important modulators of metabolic activity in
57 mammals and alter cholesterol and fatty acid levels through binding and activation of THR α s [10]. THR α s
58 exist as two subtypes, THR α and THR β , which are found in most tissues, but are differentially expressed
59 [11]; THR α is highly expressed in bone and the heart, while THR β is the major form in the liver. THR α s form
60 homodimers or heterodimerize with other nuclear receptors (e.g. retinoid X receptors, RXRs) that recognize
61 and bind thyroid hormone response elements (TREs) located in the upstream promoter region of target
62 genes. Upon ligand-binding, these complexes can activate or repress transcription directly, through
63 interaction with other transcription factors, and/or *via* the recruitment of co-activators [12-14]. Here, we have

64 characterized how THR-dependent transcription is upregulated by several thyromimetics that have reached
65 human clinical testing for the treatment of NASH: GC-1 (sobetirome, Fig 1B), MGL-3196 (resmetirom, Fig
66 1C), and VK2809, a liver-targeting prodrug that is cleaved into its active parent VK2809A by cytochrome
67 P450 isoenzyme 3A (CYP3A) after first pass intrahepatic activation (Fig 1D). GC-1 completed Phase 1
68 clinical trials in 2008 and demonstrated lipid-lowering effects with both single and multiple dosing [15], MGL-
69 3196 is in Phase 3 clinical trials and has demonstrated significant reduction in hepatic fat after 12 and 36
70 weeks of treatment [16], and VK2809 is in Phase 2 of clinical testing and has been shown to reduce hepatic
71 fat content in NAFLD patients after 12 weeks of treatment [17]. All three compounds have been reported to
72 be potent and selective activators of THR β in biochemical assays [18-20]. However, simple ligand-binding
73 assays using truncated THR proteins do not fully recapitulate the complex THR-activation cascade that
74 leads to changes in gene transcription and, ultimately, metabolic regulation. To this date, the
75 characterization of THR activation by these drug candidates using *in vitro* cell-based assays that quantify
76 gene transcription has not been reported.

77 **Fig 1. Chemical structures of test compounds**

78 Chemical structures of (A) the natural THR ligand triiodothyronine, T3, (B) sobetirome, GC-1, (C)
79 resmetirom, MGL-3196, (D) VK2809, and VK2809A, which is produced by CYP3A-mediated cleavage of
80 VK2809 after first pass intrahepatic activation.

81 In this study, we have developed a streamlined screening cascade using *in vitro* and *in vivo* systems
82 to evaluate the potency of thyromimetic candidates for the treatment of NASH. The aim of this study was
83 to compare the ability of clinically relevant THR β agonists, GC-1, MGL-3196, and VK2809, to activate their
84 cognate receptor, modulate gene expression, and, ultimately, alter cholesterol and fatty acid biosynthesis
85 and metabolism in the liver. We found that monitoring gene expression changes in human hepatocyte-
86 derived cell lines and primary human hepatocytes (PHH) provides a valuable first screen of THR β agonists
87 and accurately predicts clinical efficacy.

88

89 **Material and methods**

90 **Compounds**

91 T3 (T2877) and GC-1 (SML1900) were purchased from Sigma-Aldrich. MGL-3196, VK2809, and
92 VK2809A were synthesized by WuXi AppTec Limited (China) and compound identities and purities were
93 verified *via* high-performance liquid chromatography and liquid chromatography–mass spectrometry. All
94 compounds were dissolved in dimethyl sulfoxide (DMSO; Sigma-Aldrich, D4540)

95 **TR-FRET thyroid hormone receptor coactivator assay**

96 A time-resolved FRET (TR-FRET)-based, biochemical assay was used as an initial screen to
97 assess the ability of compounds to bind either THR α or β *in vitro*. Briefly, binding of an agonist to the GST-
98 tagged THR ligand-binding domain (LBD) causes a conformational change, resulting in higher affinity for
99 the coactivator peptide. Upon excitation of the terbium-labeled anti-GST antibody, energy is transferred to
100 the fluorescein-labeled coactivator peptide and is detected as emission at 520 nm.

101 The assay procedure is based on the manufacturer's protocol for LanthaScreen™ TR-FRET
102 Thyroid Receptor beta Coactivator Assay (Invitrogen, PV4686) with slight, optimized modifications. Briefly,
103 the assay was performed in 384-well, black microplate plates, protected from light. Test compounds were
104 serially diluted in DMSO (1.0% final DMSO concentration) and added to the test plate. GST-tagged THR α
105 or β LBD was added to the plate to yield a final concentration of 1.0 nM, followed by a mixture of the
106 fluorescein-labeled SRC2-2 coactivator peptide and terbium-labeled anti-GST antibody at the final
107 concentrations of 200.0 nM and 2.0 nM, respectively. After 90 mins incubation at room temperature (RT),
108 TR-FRET was measured on a VICTOR multilabel plate reader (Perkin Elmer) using an excitation
109 wavelength of 340 nm with 495 nm and 520 nm emission filters. The results were then quantified by
110 expressing ratios of the intensities (520:495) and dose-response curves were fitted by non-linear regression
111 with variable slope. Statistical analysis was performed in GraphPad Prism 8.0.

112 **Luciferase reporter assay in HEK293T cells**

113 After initial characterization of *in vitro* THR-binding/activation, compounds were tested for their
114 ability to bind and activate THR α or β (in complex with RXR), inducing gene expression, in cultured human-
115 derived cells. To this end, HEK293T cells were transiently transfected with a firefly luciferase reporter under
116 control of a TRE (TRE-Luc), a RXR expression plasmid, and either a THR α or β expression plasmid. This
117 assay was performed at Pharmaron Beijing Co., Ltd. (China).

118 Briefly, HEK293T cells (ATCC, CRL-3216) were seeded into 6-well culture plates at 7.0×10^5
119 cells/well and cultured in Dulbecco's Modified Eagle's Medium (DMEM; Hyclone, SH30022) supplemented
120 with 10% fetal bovine serum (FBS; Gibco, 16000-044) and 1% Penicillin-Streptomycin (P/S; Corning, 30-
121 002-CI) at 37°C and 5% CO₂. After 24 hrs of incubation, transfection complexes were prepared by mixing
122 12 μ L Lipofectamine 2000 (Invitrogen, 11668019) with 4 μ g of a plasmid mixture (1:1:4 THR:RXR:TRE-
123 Luc) in 200 μ L Opti-MEM (Invitrogen, 11058-021) and added to the cells. After overnight incubation, the
124 transfected cells were re-seeded at 1.0×10^4 cells/well into 384-well microplates and incubated for an
125 additional 5 to 6 hrs. Test compounds were serially diluted in DMSO and added to the cells (0.1% final
126 DMSO concentration). After approximately 18 to 24 hrs, the culture plates were equilibrated to RT, 30 μ L
127 ONE-Glo reagent (Promega, E6120) was added to each well, and luminescence was measured on an
128 EnSpire plate reader (Perkin Elmer). The results were then quantified by calculating percent agonism and
129 dose-response curves were fitted by non-linear regression with variable slope. Statistical analysis was
130 performed in GraphPad Prism 8.0.

131 **Differential gene expression assay in hepatic cells**

132 Huh-7 cells (JCRB Cell Bank, JCRB0403) were routinely cultured in DMEM (Corning, 10-013-CM)
133 supplemented with 10% FBS and 1% P/S at 37°C and 5% CO₂ until 80-90% confluency. Cells were then
134 detached with 0.05% trypsin (Corning, 25-052-CV), resuspended in TH-free medium (DMEM supplemented
135 with 10% TH-depleted FBS and 1% P/S), and seeded into collagen-coated, 96-well microplates (Corning,
136 354407) at 5.0×10^4 cells/well. After 24 hrs, the culture medium was replaced with treatment media. Cells

137 were treated for 24 hrs. TH-depletion of the FBS *via* resin treatment was accomplished as previously
138 described [21]. All treatment media were made by mixing test compounds, serially diluted in DMSO, with
139 TH-free medium (0.1% final DMSO concentration).

140 Transporter certified human hepatocytes (PHH) were obtained from BioIVT (Lot: JEL, F00995-
141 TCERT). Cells were thawed in Cryopreserved Hepatocytes Recovery Medium (Gibco, CM7000) and plated
142 into collagen-coated, 96-well microplates at 6.0×10^4 cells/well. After 6 hrs, the medium was replaced with
143 serum-free incubation medium, William's E Medium (Gibco, A1217601) supplemented with Primary
144 Hepatocyte Maintenance Supplements (Gibco, CM4000). After 24 hrs, the incubation medium was replaced
145 with treatment media. Cells were treated for 24 hrs. All treatment media were made by mixing test
146 compounds, serially diluted in DMSO, with serum-free incubation medium (0.1% final DMSO
147 concentration).

148 After 24 hrs in treatment media, both Huh-7 cells and PHH were processed with the TaqMan Fast
149 Advanced Cells-to-Ct Kit (Invitrogen, A35378), according to the manufacturer's protocol. Briefly, the
150 treatment media was removed and the cells were washed with 50 μ L cold 1X phosphate-buffered saline
151 (Corning, 21-040-CM). Fifty μ L lysis buffer containing DNase I was added to each well and the plate was
152 incubated on a rotor at RT for 5 mins. Five μ L stop solution was then added to each well and after another
153 2 mins incubation on a rotor at RT, the cell lysates were used for reverse transcription. The resulting cDNA
154 was diluted 1:2 with nuclease-free, distilled water (Invitrogen, 10977015). Gene expression was measured
155 using TaqMan Fast Advanced Master Mix (Applied Biosystems, 4444964) and the following TaqMan Gene
156 Expression assays (Applied Biosystems, 4331182): *18S* (Hs99999901_s1), *ACTB* (Hs01060665_g1),
157 *ANGPTL4* (Hs01101123_g1), *CPT1A* (Hs00912671_m1), *DIO1* (Hs00174944_m1), *TFG*
158 (Hs02832013_g1), *THRA* (Hs00268470_m1), and *THRB* (Hs00230861_m1). *ACTB* and *TFG* served as
159 control housekeeping genes for Huh-7 assays and *18S* and *ACTB* for PHH assays. Ten μ L reactions were
160 run on the qTOWER³ 84 (Analytik Jena). Relative quantification (RQ) of gene expression was calculated
161 *via* the $2^{-\Delta\Delta Ct}$ method and dose-response curves were fitted by non-linear regression with variable slope.
162 Statistical analysis was performed in GraphPad Prism 8.

163 **High-fat diet fed rat study**

164 Animals were purchased from Vital River Laboratory Animal Technology Co. Ltd. and experiments
165 were conducted at Covance Pharmaceutical R&D (Shanghai) Co., Ltd. (China). Animals were group-
166 housed in polycarbonate cages with corncob bedding under controlled temperature (21-25°C), humidity
167 (40-70%), and a 12-hr light/dark cycle. All procedures performed were in compliance with local animal
168 welfare legislation, Covance global policies and procedures, and the Guide for the Care and Use of
169 Laboratory Animals.

170 Male Sprague Dawley rats, approximately 8 to 11 weeks of age, were fed with either a normal diet,
171 ND (D12450K: 10 kcal% fat, no sucrose), or high-fat diet, HFD (D12109C: 40 kcal% fat, 1.25 gm%
172 cholesterol, 0.5 gm% sodium cholate, 12.5 gm% sucrose). After 12 days of diet consumption, baseline
173 serum total cholesterol and low-density lipoprotein cholesterol (LDL-C) levels were measured with the
174 cobas 6000 c501 Chemistry Analyzer (Roche) to confirm hypercholesterolemia in the HFD fed rats. Animals
175 were then randomized into treatment groups. After 14 days, serum lipid levels were re-measured (pre-dose)
176 and animals were orally dosed (P.O.) once with either vehicle (80% PEG400 in water) or MGL-3196 at 5.0
177 mg/kg, 1.5 mg/kg, or 0.5 mg/kg. T3 was administered *via* a single intraperitoneal injection (I.P.) at 0.5 mg/kg.

178 Twenty-four hrs after dosing, animals were euthanized by CO₂ inhalation and serum and plasma
179 were collected along with liver tissue. Serum total cholesterol and LDL-C levels were determined as
180 described above and concentrations of compounds were measured using liquid chromatography-tandem
181 mass spectrometry (LC-MS/MS). Tissue samples were stored in RNA later (Invitrogen, AM7020) at -70°C
182 until homogenization with the Scientz-48 TissueLyser LT. RNA extraction was performed at WuXi AppTec
183 (Hong Kong) Limited (China) with the RNeasy Mini Kit (Qiagen, 74106) and RNA concentration and quality
184 was determined using the Nanodrop 2000 (Thermo Scientific); additional quality control was assessed with
185 agarose gel electrophoresis. One μg total RNA from each sample was then reverse-transcribed using the
186 High Capacity cDNA Reverse Transcription kit (Applied Biosystems, 4368814) and the resulting cDNA was
187 diluted 1:5 with nuclease-free, distilled water. Gene expression was measured using TaqMan Fast
188 Advanced Master Mix and the following TaqMan Gene Expression assays: *Actb* (Rn00667869_m1), *Cpt1a*

189 (Rn00580702_m1), *Dio1* (Rn00572183_m1), *Me1* (Rn00561502_m1), *Rplp1* (Rn03467157_gH), and
190 *Thrsp* (Rn01511034_m1). *Actb* and *Rplp1* served as control housekeeping genes. Ten μ L reactions were
191 run on the qTOWER³ 84. Relative quantification (RQ) of gene expression was calculated *via* the $2^{-\Delta\Delta Ct}$
192 method and statistical analysis was performed in GraphPad Prism 8.0.

193 **Ethics statement**

194 Experiments involving rats were conducted at Covance Pharmaceutical R&D (Shanghai) Co., Ltd.
195 All procedures performed were in compliance with local animal welfare legislation, Covance global policies
196 and procedures, and the Guide for the Care and Use of Laboratory Animals. Animals were euthanized by
197 CO₂ inhalation.

198

199 Results

200 Characterization of THR α and THR β activation

201 Due to the significant and broad role of THs in human development and physiology, a desirable
 202 property of NASH therapeutic thyromimetics is that their action be focused to the liver in order to decrease
 203 the risk of adverse, off-target effects on the heart, bone, and muscle [22]. This can be achieved by either
 204 targeting a compound to the liver or by increasing its selectivity for THR β compared to THR α . Using a
 205 biochemical approach, the TR-FRET thyroid hormone receptor coactivator assay, and a cell-based
 206 approach, the HEK293T luciferase reporter assay, we characterized the ability of compounds to bind and
 207 activate each THR subtype. The EC₅₀ value calculated from each dose-response curve measures the
 208 potency by which a compound activates either THR; a large THR α EC₅₀-to-THR β EC₅₀ ratio (α : β) indicates
 209 increased selectivity towards THR β (Table 1).

210 **Table 1. THR α / β EC₅₀ values and selectivity of test compounds**

Compound	TR-FRET assay			Luciferase reporter assay		
	THR α EC ₅₀ (nM) Mean \pm SEM	THR β EC ₅₀ (nM) Mean \pm SEM	α : β	THR α EC ₅₀ (nM) Mean \pm SEM	THR β EC ₅₀ (nM) Mean \pm SEM	α : β
T3	0.3 \pm 0.0 (n = 54)	0.4 \pm 0.0 (n = 54)	0.8	14.3 \pm 0.6 (n = 28)	11.5 \pm 0.6 (n = 27)	1.2
GC-1	0.4 \pm 0.1 (n = 3)	0.4 \pm 0.1 (n = 3)	0.9	9.8 \pm 0.6 (n = 29)	4.6 \pm 0.3 (n = 35)	2.1
MGL-3196	933.8 \pm 175.2 (n = 7)	73.1 \pm 9.3 (n = 7)	12.8	5927.4 \pm 1117.6 (n = 3)	2365.8 \pm 689.5 (n = 4)	2.5
VK2809A	25.5 \pm 7.0 (n = 3)	10.1 \pm 2.7 (n = 3)	2.5	297.4 \pm 41.4 (n = 4)	269.0 \pm 30.9 (n = 5)	1.1
VK2809	253.2 \pm 40.7 (n = 3)	459.5 \pm 163.4 (n = 3)	0.6	54.8 \pm 11.7 (n = 4)	690.3 \pm 28.6 (n = 5)	0.1

211 In the TR-FRET thyroid hormone receptor coactivator assay, increasing concentrations of each compound
 212 was combined with the GST-tagged LBD of THR α or β , a coactivator peptide, and terbium-labeled anti-
 213 GST antibody. TR-FRET was then measured and dose-response curves were generated. In the luciferase
 214 reporter assay, HEK293T cells were transfected with a firefly luciferase reporter plasmid under the control
 215 of the TRE-Luc, a RXR expression plasmid, and either a THR α or β expression plasmid. The cells were
 216 then treated with increasing concentrations of each compound. Luminescence was measured and dose-

217 response curves were generated. For both assays, calculated EC_{50} means \pm SEM, n, and $THR\alpha$ EC_{50} -to-
218 $THR\beta$ EC_{50} ratios ($\alpha:\beta$) are reported for each compound-THR subtype combination.

219 In the TR-FRET assay, T3 showed high-affinity for both THR subtypes with no selectivity ($THR\alpha$
220 EC_{50} = 0.3 nM, $THR\beta$ EC_{50} = 0.4 nM, $\alpha:\beta$ = 0.8), as did GC-1 ($THR\alpha$ EC_{50} = 0.4 nM, $THR\beta$ EC_{50} = 0.4 nM,
221 $\alpha:\beta$ = 0.9). VK2809 was a weak binder of both THRs and showed no selectivity ($THR\alpha$ EC_{50} = 253.2 nM,
222 $THR\beta$ EC_{50} = 459.5 nM, $\alpha:\beta$ = 0.6), while VK2908A was relatively potent and slightly selective for $THR\beta$
223 ($THR\alpha$ EC_{50} = 25.5 nM, $THR\beta$ EC_{50} = 10.1 nM, $\alpha:\beta$ = 2.5) and MGL-3196 was the most $THR\beta$ selective
224 compound tested, although its potency was relatively low ($THR\alpha$ EC_{50} = 993.8 nM, $THR\beta$ EC_{50} = 73.1 nM,
225 $\alpha:\beta$ = 12.8).

226 Next, we tested whether the compounds would behave similarly in a less artificial system by
227 indirectly measuring gene transcription changes in a cellular context with a luciferase reporter assay in
228 HEK293T cells. In this assay, T3 remained a very potent compound, with no selectivity ($THR\alpha$ EC_{50} = 14.3
229 nM, $THR\beta$ EC_{50} = 11.5 nM, $\alpha:\beta$ = 1.2) and GC-1 was also potent with marginal $THR\beta$ selectivity ($THR\alpha$
230 EC_{50} = 9.8 nM, $THR\beta$ EC_{50} = 4.6 nM, $\alpha:\beta$ = 2.1). VK2809 showed increased potency for $THR\alpha$ ($THR\alpha$ EC_{50}
231 = 54.8 nM, $THR\beta$ EC_{50} = 690.3 nM, $\alpha:\beta$ = 0.1), while VK2809A was considerably less potent compared to
232 its previous characterization ($THR\alpha$ EC_{50} = 297.4 nM, $THR\beta$ EC_{50} = 269.0 nM, $\alpha:\beta$ = 1.1). MGL-3196 was a
233 considerably weaker binder and activator of both THRs with reduced $THR\beta$ selectivity in this assay ($THR\alpha$
234 EC_{50} = 5927.4 nM, $THR\beta$ EC_{50} = 2365.8 nM, $\alpha:\beta$ = 2.5) compared to the TR-FRET assay.

235 Although both *in vitro* assays provided preliminary information on how these compounds behave,
236 neither system is ideal. The TR-FRET assay presents a highly artificial environment using truncated
237 versions of the THRs and the HEK293T luciferase reporter assay measures transcription indirectly *via*
238 luciferase activity in a non-hepatocyte-derived cell-line that is overexpressing either receptor subtype.

239 **Differential gene expression analysis of direct THR targets in** 240 **human hepatic cells**

241 We aimed to develop an *in vitro*, cell-based assay that is not only amenable to high throughput
242 screening of compounds, but that can also more reliably recapitulate *in vivo* processes. Because activated
243 THR may function as a transcription factor, we compared the action of THR agonists in a human
244 hepatocyte-derived cell line and in primary human hepatocytes (PHH) by quantifying transcriptional
245 changes resulting from compound treatment (Fig 2A). Cells were cultured in TH-depleted media for 24 hrs
246 and then treated with compounds for 24 hrs. The RNA levels of THR target genes were then measured *via*
247 RT-qPCR.

248 **Fig 2. Differential gene expression in Huh-7 cells and PHH resulting from treatment with THR**
249 **agonists**

250 (A) Illustration of the *in vitro*, hepatic cell-based differential gene expression assay design. (B) *THRB* and
251 *THRA* RNA levels were quantified by RT-qPCR in HepG2 (n = 3), Huh-7, (n = 3), and PHH (n = 5) cells.
252 Mean RQ values \pm SEM are reported with means annotated within the bars. (C) Huh-7 cells were treated
253 with increasing doses of T3 (n = 2), GC-1 (n = 2), or MGL-3196 (n = 2) for 24 hrs. *ANGPLT4*, *CPT1A*, and
254 *DIO1* RNA levels were quantified by RT-qPCR and dose-response curves were generated for each gene-
255 compound combination. Mean EC₅₀ values (red bar) and individual replicate EC₅₀ values (black symbols)
256 are reported. (D) Huh-7 cells were treated with increasing doses of T3 (black), GC-1 (red), MGL-3196
257 (green), VK2809A (solid blue), or VK2809 (dashed blue) for 24 hrs. *CPT1A* RNA levels were quantified by
258 RT-qPCR. Representative mean RQ values at each compound concentration and fitted dose-response
259 curves are reported. (E) PHH were treated with increasing doses of T3 (black), GC-1 (red), MGL-3196
260 (green), VK2809A (solid blue), or VK2809 (dashed blue) for 24 hrs. *THRSP* RNA levels were quantified by
261 RT-qPCR. Representative mean RQ values at each compound concentration and fitted dose-response
262 curves are reported. (F) EC₅₀ values for every test compound were calculated from dose-response curves
263 generated from the TR-FRET THR β , luciferase (Luc) reporter THR β , Huh-7 differential gene expression
264 (RQ), and PHH RQ assays (data reported in Tables 1 and 2). Mean EC₅₀ values \pm SEM are reported.

265 To choose the most appropriate cell line for the assay, THR expression levels in HepG2 and Huh-
266 7 cells were quantified *via* RT-qPCR. While both cell lines expressed more *THRB* than *THRA*, reflecting
267 the expression patterns observed in liver tissue [23-26], Huh-7 cells had a larger *THRB*-to-*THRA* ratio, 2.9

268 compared to 1.7 for HepG2, and was thus used in downstream assays (Fig 2B). We then tested the effects
269 of T3, GC-1, and MGL-3196 on the expression of several known THR gene targets. Treatment with these
270 compounds resulted in dose-dependent increases in *ANGPTL4*, *CPT1A*, and *DIO1* transcript levels (S1A-
271 C Figs). EC₅₀ values were calculated from the resulting dose-response curves and used as a measure of
272 potency (Fig 2C). Across the three gene targets, T3 was the most potent activator of THR (mean EC₅₀ (nM):
273 *ANGPTL4* = 1.3, *CPT1A* = 0.7, *DIO1* = 1.2), followed by GC-1 (mean EC₅₀ (nM): *ANGPTL4* = 6.2, *CPT1A*
274 = 1.9, *DIO1* = 3.6), and MGL-3196 was the least potent compound tested (mean EC₅₀ (nM): *ANGPTL4* =
275 508.4, *CPT1A* = 308.0, *DIO1* = 245.8). *CPT1A* transcription was ultimately chosen as the endpoint for
276 downstream screening assays as the gene is known to be highly transcribed in the liver, a direct target of
277 THR [27, 28], and its transcript levels were the most abundant in Huh-7 cells compared to *ANGPTL4* and
278 *DIO1* (i.e. lowest mean Ct value; S1D Fig). This gene encodes the enzyme, carnitine palmitoyltransferase
279 1A, which has an essential role in mitochondrial fatty acid β-oxidation [29, 30]. Next, we expanded testing
280 to include other THR agonists, VK2809 and VK2809A. All compounds caused dose-dependent increases
281 in *CPT1A* expression, but with disparate potencies (Fig 2D). EC₅₀ values indicate that T3 was the most
282 potent activator of THR, followed by GC-1, VK2809A, MGL-3196, then VK2809 (Table 2; mean Huh-7 EC₅₀
283 (nM): 0.3, 1.3, 8.3, 303.1, and 589.1, respectively).

284 **Table 2. Differential gene expression assay EC₅₀ values in Huh-7 cells and PHH**

Compound	Huh-7 EC ₅₀ (nM)	PHH EC ₅₀ (nM)
	Mean ± SEM	Mean ± SEM
T3	0.3 ± 0.03 (n = 22)	1.0 ± 0.6 (n = 4)
GC-1	1.3 ± 0.2 (n = 5)	2.7 ± 1.6 (n = 4)
MGL-3196	303.1 ± 50.9 (n = 17)	216.2 ± 197.5 (n = 3)
VK2809A	8.3 ± 2.2 (n = 5)	14.8 ± 10.7 (n = 4)
VK2809	589.1 ± 120.1 (n = 5)	18.7 ± 8.9 (n = 3)

285 Huh-7 cells and PHH were treated with increasing concentrations of each compound and resulting
286 differential gene expression was measured and quantified as described in Figs 2D and 2E, respectively.
287 Calculated EC₅₀ means ± SEM and n are reported for each compound-cell type combination.

288 We next sought to validate the characterizations of these THR agonists in a more relevant cellular
289 model, PHH. Like Huh-7 cells and liver tissue, PHH expressed 4.2-times more *THRB* than *THRA* (Fig 2B).
290 In PHH, treatment with the THR agonists resulted in increased expression of a direct THR gene target,
291 *THRSP* (Fig 2E), which encodes thyroid hormone responsive protein and promotes lipogenesis [31, 32].
292 Four out of the five compounds tested showed comparable EC₅₀ values and maintained relative potencies
293 between the two cellular models and two target genes (Fig 2F and Table 2; mean PHH EC₅₀ (nM): T3 =
294 1.0, GC-1 = 2.7, VK2809A = 14.8, MGL-3196 = 216.2), confirming the robustness of these assays. The one
295 exception was VK2809 (mean PHH EC₅₀ = 18.7 nM), which had significantly increased potency that was
296 almost equal to that of VK2809A in PHH.

297 ***In vivo* modulation of serum lipid levels and liver gene** 298 **expression**

299 We examined whether modulation of gene expression by these thyromimetics would translate into
300 physiological alterations in metabolism. The most and least potent compounds as characterized by the *in*
301 *vitro* assays, T3 and MGL-3196, respectively, were chosen to be tested *in vivo* (Fig 3A).
302 Hypercholesterolemia was induced in rats by feeding with a HFD for two weeks. The rats were then treated
303 with a single dose of compound and serum lipid levels and liver gene expression were quantified. *Dio1* and
304 *Me1* are highly expressed in the liver and are known targets of THR [33-36]. DIO1, iodothyronine deiodinase
305 1, is a selenoprotein that functions to regulate circulating levels of T3 by catalyzing the conversion of T4
306 into T3 and of T3 into T2 [37, 38]. ME1, malic enzyme 1, is a NADP-dependent enzyme that generates
307 NADPH for fatty acid biosynthesis [39, 40].

308 **Fig 3. Modulation of serum lipid levels after a single-dose treatment of MGL-3196 or T3 in HFD fed** 309 **rats**

310 (A) Illustration of *in vivo* study design. (B) After two weeks of ND or HFD consumption and before compound
311 treatment, total cholesterol levels of all animals were measured. Animals were then randomized into
312 treatment groups: ND: vehicle (n = 20); HFD: vehicle (n = 20), 5.0 mg/kg MGL-3196 (n = 12), 1.5 mg/kg

313 MGL-3196 (n = 20), 0.5 mg/kg MGL-3196 (n = 6), and 0.5 mg/kg T3 (n = 6). Total cholesterol level means
314 \pm SEM are reported. Statistical analysis was performed using Brown-Forsythe and Welch ANOVA and the
315 mean of each group was compared to the mean of every other group; 'a' is statistically significant from 'b'
316 with $P < 0.01$. (C) LDL-C was measured in the same animals described in B). LDL-C level means \pm SEM
317 are reported. Statistical analysis was performed using Brown-Forsythe and Welch ANOVA tests and the
318 mean of each group was compared to the mean of every other group; 'a' is statistically significant from 'b'
319 with $P < 0.01$. (D) The rats described above were then dosed once with their assigned treatments. Twenty-
320 four hrs later, total cholesterol levels of all animals were measured. Results are presented as percent
321 change between pre-dose and post-dose total cholesterol levels of individual animals. Percent change
322 means \pm SEM are reported with mean values annotated within the bars. Statistical analysis was performed
323 using Brown-Forsythe and Welch ANOVA tests and the mean of each group was compared to the mean of
324 the HFD fed, vehicle-control group; **** $P < 0.0001$. (E) LDL-C measurements were obtained from the same
325 rats described in D). Results are presented as percent change between pre-dose and post-dose LDL-C
326 levels of individual animals. Percent change means \pm SEM are reported with mean values annotated within
327 the bars. Statistical analysis was performed using Brown-Forsythe and Welch ANOVA tests and the mean
328 of each group was compared to the mean of the HFD fed, vehicle-control group; * $P < 0.05$, **** $P < 0.0001$.
329 (F) Plasma compound concentration in MGL-3196-treated animals was determined using LC-MS/MS.
330 Results are presented as the mean plasma $AUC_{0-24hrs}$ with mean values annotated above the bars.

331 After two weeks of feeding and prior to dosing compounds, total cholesterol and LDL-C levels were
332 significantly elevated in HFD fed rats compared to ND fed rats, but there were no significant differences in
333 either endpoint among the HFD groups (Figs 3B and C). Analysis comparing serum lipid levels within the
334 same individual animals pre-dose and 24 hrs post-dose revealed that treatment with 0.5 mg/kg T3
335 decreased total cholesterol by 68.2%, to levels comparable to that of ND fed rats, while MGL-3196 dose-
336 dependently decreased total cholesterol, with 5 mg/kg yielding a maximal decrease of 33.6% and 0.5 mg/kg
337 having no significant effect (Fig 3D and S2A Fig). Similar trends were observed for LDL-C levels (Fig 3E
338 and S2B Fig). Further analysis comparing serum lipid levels of drug-treated animals to those of HFD fed,
339 vehicle-control animals revealed similar concentration-dependent reductions by MGL-3196 and a drastic
340 decrease by T3 (S2C and D Figs). Moreover, pharmacokinetic analysis confirmed that exposure to MGL-

341 3196, as measured by the area-under-the-plasma-drug-concentration-time curve (plasma $AUC_{0-24hrs}$), was
342 indeed linearly dose-dependent (Fig 3F).

343 We hypothesized that concurrent with the changes in serum lipid levels were alterations in liver
344 gene expression induced by MGL-3196 and T3 activation of THR. Initial experiments were performed to
345 identify reliable genetic endpoints from a panel of known THR targets, which included *Cpt1a*, *Dio1*, *Me1*,
346 and *Thrsp*. The RNA levels of these targets were quantified in livers of HFD fed rats 4 or 24 hrs after dosing
347 with either 5.0 or 1.5 mg/kg MGL-3196. After 4 hrs, MGL-3196 activated the transcription of *Cpt1a*, *Dio1*,
348 and *Thrsp* in a dose-dependent manner, with increases in *Thrsp* levels being the most robust; there was
349 no significant increase in *Me1* level compared to HFD fed, vehicle-control rats at this time (Fig 4A). At 24
350 hrs after dosing, the increases in RNA levels were dampened for *Cpt1a* and *Thrsp* (Fig 4B). By this time,
351 however, transcription of *Dio1* and *Me1* was significantly increased with MGL-3196 treatment in a dose-
352 dependent manner compared to HFD fed, vehicle-control rats (Fig 4B). Consequently, the expression of
353 *Dio1* and *Me1* 24 hrs after dosing were chosen as the endpoints in subsequent experiments as these
354 options offered the most consistent and robust responses when dosing with a thymomimetic.

355 **Fig 4. Modulation of liver gene expression after single-dose treatment of MGL-3196 or T3 in HFD fed**
356 **rats**

357 (A) After two weeks of consuming a HFD, animals were dosed once with vehicle (n = 6), 5.0 mg/kg MGL-
358 3196 (n = 3), or 1.5 mg/kg MGL-3196 (n = 3). Four hrs later, the animals were sacrificed and liver *Cpt1a*,
359 *Dio1*, *Me1*, and *Thrsp* RNA levels were quantified by RT-qPCR. Results are presented as expression
360 relative to the expression levels in vehicle-control rats. Mean RQ values \pm SEM are reported. (B) Animals
361 were treated as in A) except that they were sacrificed 24 hrs post-dosing and gene expression analysis
362 was conducted in the same manner. Results are presented as expression relative to the expression levels
363 in vehicle-control rats. Mean RQ values \pm SEM are reported. (C) The rats described in Fig 3 were sacrificed
364 24 hrs after compound treatment and liver *Dio1* RNA levels were quantified by RT-qPCR. Results are
365 presented as expression relative to the expression levels in HFD fed, vehicle-control rats. Mean RQ values
366 \pm SEM are reported with mean values annotated within the bars. Statistical analysis was performed using
367 Brown-Forsythe and Welch ANOVA tests on the $\Delta\Delta C_t$ values. The mean of each group was compared to

368 the mean of the HFD fed, vehicle-control group; **P < 0.01, ****P < 0.0001. (D) Liver *Me1* expression was
369 quantified in the same rats as described in C) and in the same manner. Results are presented as expression
370 relative to the expression levels in HFD fed, vehicle-control rats. Mean RQ values \pm SEM are reported with
371 mean values annotated within the bars. Statistical analysis was performed using Brown-Forsythe and
372 Welch ANOVA tests on the $\Delta\Delta$ Ct values. The mean of each group was compared to the mean of the HFD
373 fed, vehicle-control group; *P < 0.05, **P < 0.01, ****P < 0.0001.

374 Liver *Dio1* and *Me1* RNA levels were quantified in the same animals whose serum lipid levels were
375 reported in Fig 3. From these data, we were able to compare the abilities of MGL-3196 and T3 to activate
376 THR and modulate gene transcription *in vivo*. A single dose of 0.5 mg/kg T3 resulted in a 4.3-fold increase
377 in liver *Dio1* expression compared to the vehicle, while a single dose of MGL-3196 resulted in concentration-
378 dependent increases in liver *Dio1* expression, with 5 mg/kg yielding the maximal 1.9 fold-increase and 0.5
379 mg/kg having no significant effect compared to the HFD fed, vehicle-control group (Fig 4C). Similar trends
380 were observed for liver *Me1* expression (Fig 4D).

381 In summary, treatment with MGL-3196 and T3 in HFD fed rats resulted in reduced serum lipid levels
382 that mirrored increased gene expression levels in the liver. Furthermore, we observed dose-dependent
383 changes of these parameters with MGL-3196 treatment, which showed significantly weaker potency than
384 T3 in the biochemical assay, cell-based assays, and in the HFD fed rat model. These results confirm that
385 the *in vitro* characterizations of these THR agonists can be recapitulated *in vivo* and the effects of these
386 agonists can be quantified by measuring physiological (serum lipid levels) as well as molecular (gene
387 expression) endpoints.

388

389 Discussion

390 While many studies highlight lipid level changes in animal models when profiling NAFLD/NASH
391 therapeutic candidates, *in vitro* testing of compounds in human hepatocytes is a system that offers valuable,
392 precursory information faster and with higher throughput. We have implemented a strategy to rank the
393 efficacy of THR β agonists by quantifying changes in the transcription of genes that lead to metabolic
394 alterations, an effect that is directly downstream of THR binding and activation.

395 In the TR-FRET assay, GC-1 proved to be the most effective thyromimetic, with THR α / β EC₅₀
396 values comparable to T3, followed by VK2908A, and MGL-3196 was a weak activator of either THR subtype
397 (Table 1). The results also indicate that MGL-3196 was the most THR β -selective thyromimetic (α : β = 12.8)
398 and that GC-1 and VK2809A had no or minimal THR β selectivity (α : β = 0.9 and 2.5, respectively). These
399 findings are contrary to previously published results that describe GC-1 as having approximately 3- to 10-
400 fold selectivity [18, 41, 42] and VK2908A (MB07344) as having 15.8-fold selectivity for THR β over THR α
401 [43]. These discrepancies may be explained by the fact that the other studies derived selectivity from only
402 ligand-binding affinities (K_d or K_i), while the TR-FRET assay also considers coactivator recruitment, which
403 is more physiologically relevant and a measure of receptor agonism. This type of cell-free, coactivator
404 recruitment assay has been employed by Kelly *et al.* to characterize a variety of thyroid hormone analogues
405 [19]. In that same study, the authors found MGL-3196 (compound 53) to be 28.3-fold more selective for
406 THR β over THR α , which is greater than what we observed for the compound (α : β = 12.8). This disparity
407 could be due differences in data reporting. While we calculate selectivity as the crude THR α EC₅₀-to-THR
408 β EC₅₀ ratio (α : β), Kelly *et al.* normalized this value by the selectivity of T3 from each assay. Furthermore,
409 they reported relatively wide ranges of THR- β and THR- α values (THR- β = 0.024-0.12 μ M; THR- α = 0.003-
410 0.10 μ M) compared to data reported in this current study (Table 1), which may skew their compound
411 selectivity calculations. Other researchers using the same coactivator recruitment assay, published in a
412 recent study data on T3, MGL-3196, and VK2809A that were consistent with our findings [44]. Kirschberg
413 *et al.* characterized T3 and VK2809A as having no and minimal selectivity for THR β (α : β = 1 and 2.1,
414 respectively), while MGL-3196 had a selectivity value of 15, confirming the characterizations presented in

415 our current study. Finally, the rankings of compound potency and THR β selectivity as determined by the
416 TR-FRET assay were conserved in the luciferase reporter assay for the majority of compounds tested, but
417 all THR β potencies were decreased in the luciferase reporter assay, especially that of MGL-3196 (Table 1
418 and Fig 2F).

419 Primary *in vitro* screens such as the TR-FRET and luciferase reporter assays provide general
420 trends as to how test compounds may interact with THRs. However, we recognize that these approaches
421 rely on heavily manipulated features and may not accurately reflect molecular interactions and activities
422 occurring in hepatocytes. For example and as described above, MGL-3196 showed lower THR β potency
423 in the luciferase reporter assay in HEK293T cells compared to the biochemical, TR-FRET assay (32.4-fold
424 decrease, Table 1). Furthermore, MGL-3196 was 7.8- and 10.9-times less potent in the THR β luciferase
425 reporter assay than in the Huh-7 and PHH gene expression assays, respectively (Fig 2F). This is due to
426 the fact that MGL-3196 is a liver-directed drug, being a substrate for hepatic OATP1B1/B3 transporters
427 [45]. Because these transporters are not expressed in the embryonic kidney-derived HEK293T cells, the
428 luciferase reporter assay neglects this key feature of the compound, while the cell-free TR-FRET assay
429 circumvents any cellular limitations. By quantifying RNA levels in human hepatocytes using RT-qPCR, we
430 can observe gene expression changes that are directly downstream of THR-binding and activation, in a
431 model that is more biologically relevant. However, THR subtype selectivity cannot be assessed in this more
432 natural system.

433 Since employing PHH may be resource-prohibitive for many researchers, hepatocellular carcinoma
434 (HCC) cell lines that express more *THRB* than *THRA*, such as Huh-7 cells (Fig 2B), are suitable alternatives.
435 Furthermore, EC₅₀ values from the Huh-7 differential gene expression assay were less variable than those
436 derived from the PHH assay (Fig 2F). However, using immortalized cell lines is associated with several
437 known caveats. In the Huh-7 assay, the prodrug VK2809 was characterized as weak activator of THR, 71-
438 times weaker than its active parent phosphonate VK2809A (Table 2). VK2809 in PHH, however, showed
439 drastically increased potency comparable to that of VK2809A (Fig 2F). This observation can be explained
440 by the facts that CYP3A catalyzes the cleavage of VK2809 into VK2809A in the liver [43] and that HCC-
441 derived cell lines have reduced CYP450 expression compared to primary hepatocytes [46]. We propose

442 that the ineffectiveness of VK2809 in Huh-7 cells was due to the model's decreased ability to cleave the
443 prodrug into the active form that could then bind THR and activate gene transcription. Alternatively, in PHH,
444 VK2809 was efficiently metabolized and, therefore, showed similar potency to VK2089A. Therefore, while
445 HCC cell lines are an efficient system that is amenable to high-throughput screening of compounds, we
446 recommend secondary testing of candidate thymomimetics in PHH to verify initial potency observations.
447 These findings taken together support the use of the described Huh-7 differential gene expression assay
448 to screen for THR agonist activity, with PHH providing increased biological relevance and additional
449 validation. Overall, the potencies of test compounds as measured by EC₅₀ were consistent across the *in*
450 *vitro* assays employed in this study (Fig 2F), and the few inconsistencies were readily explained by
451 limitations of the specific models.

452 We applied our preclinical screening approach to the two most advanced THR agonists in clinical
453 development for the treatment of NASH, MGL-3196 (resmetirom), and VK2809(A). Our aim was to
454 determine whether the behavior of MGL-3196 and VK2809(A) in our established *in vitro* and *in vivo* models
455 were predictive of their effects in humans. To this date, the characterization of THR-mediated transcription
456 activation by these two drug candidates using *in vitro* cell-based assays has not been reported. Gene
457 expression upregulation by GC-1 in HepG2 cells has been previously described [23], but clinical testing of
458 this compound for the treatment of NASH has been suspended for several years and is unlikely to resume
459 in the near future [47]. Treatment of healthy volunteers for two weeks with MGL-3196 dosed at ≥ 80 mg
460 resulted in 16.0-22.8% and 21.8-30.3% reduction in total and LDL-C, respectively [48]. By comparison, 14-
461 day treatment with ≥ 5 mg of VK2809 reduced LDL-C by up to 41.2% [49]. In NASH patients, 12 weeks of
462 treatment with MGL-3196 achieved a relative reduction in hepatic fat of approximately 36% as measured
463 by magnetic resonance imaging-derived proton density fat fraction [16], while relative reductions in liver fat
464 were between 53.8 and 59.7% with VK2809, depending on the dosing regimen ranging from 5-10 mg [17].
465 To elucidate the underlying molecular mechanisms contributing to the differences in clinical efficacy
466 between the two molecules, we employed our described *in vitro* screening tools. In both the TR-FRET and
467 luciferase reporter assays, the active parent phosphonate VK2809A was 7.2- to 8.8-times more potent than
468 MGL-3196 at binding and activating THR β (Table 1). This observation was confirmed in Huh-7 cells and in
469 PHH, where VK2809A was 14.6- to 36.5-times more potent than MGL-3196 at activating gene transcription

470 (Table 2). Taken together, these results confirm the ability of our *in vitro* screening methods to rapidly
471 predict the efficacy of THR agonists in human clinical research.

472 Previous studies using a cholesterol-fed rat model showed that a single-dose of 0.5 mg/kg VK2809
473 (compound 72) resulted in a 36% reduction in total cholesterol, with up to a 55% decrease at 3.0 mg/kg
474 [20]. In our present HFD fed rat study, a single-dose of 0.5 mg/kg of MGL-3196 did not significantly lower
475 total or LDL-C levels (Figs 3D-E). MGL-3196 showed a dose-dependent decrease in total cholesterol
476 starting at 1.5 mg/kg, with 5 mg/kg yielding a maximal decrease of 33.6% (Fig 3D). In comparison, a single
477 dose of 0.5 mg/kg T3 resulted in a 68.2% decrease in total cholesterol. These results reinforce that
478 observations that MGL-3196 has less pronounced cholesterol-lowering effects than what has been reported
479 for VK2809. Furthermore, the cholesterol levels did not decrease linearly with MGL-3196 doses and
480 exposures. A three-fold increase in dose, 1.5 to 5.0 mg/kg, resulted in a 2.6-fold increase in exposure (Fig
481 3F), but only in a 1.3-fold decrease in serum total cholesterol (Fig 3D). This plateauing effect in cholesterol
482 reduction observed in rats is reminiscent of the lack of a linear dose-dependent cholesterol response
483 observed in the clinic [48]. Although there could be several reasons for the plateauing dose-response of
484 MGL-3196, the single-dose HFD fed rat model provides a valuable preclinical, *in vivo* endpoint that may
485 predict the metabolic response in humans.

486 Finally, we determined that the serological effect on lipids correlates well with changes in gene
487 expression in the liver (Fig 4). *Dio1* and *Me1* RNA levels were sensitive biomarkers of liver THR activation,
488 with significant activation observed at 1.5 and 5.0 mg/kg MGL-3196. Again, the magnitude of MGL-3196-
489 induced transcription was lower compared to the effect of T3, and the increase in liver *Dio1* expression
490 between 1.5 and 5 mg/kg of MGL-3196 was only 1.3-fold (Fig 4C). Furthermore, VK2809 treatment in mice
491 has been shown to increase the expression of CPT1A [50], a gene that we have confirmed as THR target
492 in both Huh-7 cells and in rat liver (Fig 2D and 4A). Taken together, our *in vitro* and *in vivo* results comparing
493 clinically relevant molecules provide a roadmap for the rapid screening of potent and selective liver targeting
494 THR β agonists for the potential treatment of NAFLD and NASH.

495

496 **Acknowledgments**

497 Selected work was conducted at Covance Pharmaceutical R&D (Shanghai) Co., Ltd. by Peng Tu
498 et al., Pharmaron Beijing Co., Ltd. by Xiaofen Guo et al., and WuXi AppTec (Hong Kong) Limited by Xin
499 Chen, Shuang Ding, et al. We would like to thank these teams for successful collaborations.

500 **References**

- 501
502 1. Perumpail BJ, Khan MA, Yoo ER, Cholankeril G, Kim D, Ahmed A. Clinical epidemiology and
503 disease burden of nonalcoholic fatty liver disease. *World J Gastroenterol.* 2017;23(47):8263-76. doi:
504 10.3748/wjg.v23.i47.8263. PubMed PMID: 29307986; PubMed Central PMCID: PMC5743497.
- 505 2. Anstee QM, Targher G, Day CP. Progression of NAFLD to diabetes mellitus, cardiovascular
506 disease or cirrhosis. *Nat Rev Gastroenterol Hepatol.* 2013;10(6):330-44. Epub 2013/03/19. doi:
507 10.1038/nrgastro.2013.41. PubMed PMID: 23507799.
- 508 3. Younossi ZM, Koenig AB, Abdelatif D, Fazel Y, Henry L, Wymer M. Global epidemiology of
509 nonalcoholic fatty liver disease-Meta-analytic assessment of prevalence, incidence, and outcomes.
510 *Hepatology.* 2016;64(1):73-84. Epub 2016/02/22. doi: 10.1002/hep.28431. PubMed PMID: 26707365.
- 511 4. Attia SL, Softic S, Mouzaki M. Evolving role for pharmacotherapy in NAFLD/NASH. *Clin Transl Sci.*
512 2020. Epub 2020/06/25. doi: 10.1111/cts.12839. PubMed PMID: 32583961.
- 513 5. Eshraghian A. Current and emerging pharmacological therapy for non-alcoholic fatty liver disease.
514 *World J Gastroenterol.* 2017;23(42):7495-504. doi: 10.3748/wjg.v23.i42.7495. PubMed PMID: 29204050;
515 PubMed Central PMCID: PMC5698243.
- 516 6. Musso G, Cassader M, Gambino R. Non-alcoholic steatohepatitis: emerging molecular targets and
517 therapeutic strategies. *Nat Rev Drug Discov.* 2016;15(4):249-74. Epub 2016/01/22. doi:
518 10.1038/nrd.2015.3. PubMed PMID: 26794269.
- 519 7. Kim KH, Lee MS. Pathogenesis of Nonalcoholic Steatohepatitis and Hormone-Based Therapeutic
520 Approaches. *Front Endocrinol (Lausanne).* 2018;9:485. Epub 2018/08/24. doi: 10.3389/fendo.2018.00485.
521 PubMed PMID: 30197624; PubMed Central PMCID: PMC6117414.
- 522 8. Jakobsson T, Vedin LL, Parini P. Potential Role of Thyroid Receptor β Agonists in the Treatment
523 of Hyperlipidemia. *Drugs.* 2017;77(15):1613-21. doi: 10.1007/s40265-017-0791-4. PubMed PMID:
524 28865063; PubMed Central PMCID: PMC5613055.
- 525 9. Saponaro F, Sestito S, Runfola M, Rapposelli S, Chiellini G. Selective Thyroid Hormone Receptor-
526 Beta (TR β) Agonists: New Perspectives for the Treatment of Metabolic and Neurodegenerative Disorders.

- 527 Front Med (Lausanne). 2020;7:331. Epub 2020/07/09. doi: 10.3389/fmed.2020.00331. PubMed PMID:
528 32733906; PubMed Central PMCID: PMC7363807.
- 529 10. Sinha RA, Singh BK, Yen PM. Direct effects of thyroid hormones on hepatic lipid metabolism. Nat
530 Rev Endocrinol. 2018;14(5):259-69. Epub 2018/02/23. doi: 10.1038/nrendo.2018.10. PubMed PMID:
531 29472712; PubMed Central PMCID: PMC6013028.
- 532 11. Brent GA. Mechanisms of thyroid hormone action. J Clin Invest. 2012;122(9):3035-43. Epub
533 2012/09/04. doi: 10.1172/JCI60047. PubMed PMID: 22945636; PubMed Central PMCID:
534 PMC6013028.
- 535 12. Oetting A, Yen PM. New insights into thyroid hormone action. Best Pract Res Clin Endocrinol
536 Metab. 2007;21(2):193-208. doi: 10.1016/j.beem.2007.04.004. PubMed PMID: 17574003.
- 537 13. Chan IH, Privalsky ML. Isoform-specific transcriptional activity of overlapping target genes that
538 respond to thyroid hormone receptors alpha1 and beta1. Mol Endocrinol. 2009;23(11):1758-75. Epub
539 2009/07/23. doi: 10.1210/me.2009-0025. PubMed PMID: 19628582; PubMed Central PMCID:
540 PMC2775939.
- 541 14. Mengeling BJ, Lee S, Privalsky ML. Coactivator recruitment is enhanced by thyroid hormone
542 receptor trimers. Mol Cell Endocrinol. 2008;280(1-2):47-62. Epub 2007/10/06. doi:
543 10.1016/j.mce.2007.09.011. PubMed PMID: 18006144; PubMed Central PMCID: PMC2197157.
- 544 15. Scanlan TS. Sobeitrome: a case history of bench-to-clinic drug discovery and development. Heart
545 Fail Rev. 2010;15(2):177-82. Epub 2008/11/11. doi: 10.1007/s10741-008-9122-x. PubMed PMID:
546 19002578.
- 547 16. Harrison SA, Bashir MR, Guy CD, Zhou R, Moylan CA, Frias JP, et al. Resmetirom (MGL-3196)
548 for the treatment of non-alcoholic steatohepatitis: a multicentre, randomised, double-blind, placebo-
549 controlled, phase 2 trial. Lancet. 2019;394(10213):2012-24. Epub 2019/11/11. doi: 10.1016/S0140-
550 6736(19)32517-6. PubMed PMID: 31727409.
- 551 17. Loomba R, Neutel J, Mohseni R, Bernard D, Severance R, Dao M, et al. LBP-20-VK2809, a Novel
552 Liver-Directed Thyroid Receptor Beta Agonist, Significantly Reduces Liver Fat with Both Low and High
553 Doses in Patients with Non-Alcoholic Fatty Liver Disease: A Phase 2 Randomized, Placebo-Controlled

- 554 Trial. *Journal of Hepatology*. 2019;70(1, Supplement):e150-e1. doi: <https://doi.org/10.1016/S0618->
555 8278(19)30266-X.
- 556 18. Chiellini G, Apriletti JW, Yoshihara HA, Baxter JD, Ribeiro RC, Scanlan TS. A high-affinity subtype-
557 selective agonist ligand for the thyroid hormone receptor. *Chem Biol*. 1998;5(6):299-306. doi:
558 10.1016/s1074-5521(98)90168-5. PubMed PMID: 9653548.
- 559 19. Kelly MJ, Pietranico-Cole S, Larigan JD, Haynes NE, Reynolds CH, Scott N, et al. Discovery of 2-
560 [3,5-dichloro-4-(5-isopropyl-6-oxo-1,6-dihydropyridazin-3-yloxy)phenyl]-3,5-dioxo-2,3,4,5-
561 tetrahydro[1,2,4]triazine-6-carbonitrile (MGL-3196), a Highly Selective Thyroid Hormone Receptor β
562 agonist in clinical trials for the treatment of dyslipidemia. *J Med Chem*. 2014;57(10):3912-23. Epub
563 2014/04/08. doi: 10.1021/jm4019299. PubMed PMID: 24712661.
- 564 20. Boyer SH, Jiang H, Jacintho JD, Reddy MV, Li H, Li W, et al. Synthesis and biological evaluation
565 of a series of liver-selective phosphonic acid thyroid hormone receptor agonists and their prodrugs. *J Med*
566 *Chem*. 2008;51(22):7075-93. doi: 10.1021/jm800824d. PubMed PMID: 18975928.
- 567 21. Samuels HH, Stanley F, Casanova J. Depletion of L-3,5,3'-triiodothyronine and L-thyroxine in
568 euthyroid calf serum for use in cell culture studies of the action of thyroid hormone. *Endocrinology*.
569 1979;105(1):80-5. doi: 10.1210/endo-105-1-80. PubMed PMID: 446419.
- 570 22. Pedrelli M, Pramfalk C, Parini P. Thyroid hormones and thyroid hormone receptors: effects of
571 thyromimetics on reverse cholesterol transport. *World J Gastroenterol*. 2010;16(47):5958-64. doi:
572 10.3748/wjg.v16.i47.5958. PubMed PMID: 21157972; PubMed Central PMCID: PMC3007105.
- 573 23. Yuan C, Lin JZ, Sieglaff DH, Ayers SD, Denoto-Reynolds F, Baxter JD, et al. Identical gene
574 regulation patterns of T3 and selective thyroid hormone receptor modulator GC-1. *Endocrinology*.
575 2012;153(1):501-11. Epub 2011/11/08. doi: 10.1210/en.2011-1325. PubMed PMID: 22067320; PubMed
576 Central PMCID: PMC3249679.
- 577 24. Cheng SY, Leonard JL, Davis PJ. Molecular aspects of thyroid hormone actions. *Endocr Rev*.
578 2010;31(2):139-70. Epub 2010/01/05. doi: 10.1210/er.2009-0007. PubMed PMID: 20051527; PubMed
579 Central PMCID: PMC32852208.

- 580 25. Cheng SY. Multiple mechanisms for regulation of the transcriptional activity of thyroid hormone
581 receptors. *Rev Endocr Metab Disord.* 2000;1(1-2):9-18. doi: 10.1023/a:1010052101214. PubMed PMID:
582 11704997.
- 583 26. Williams GR. Cloning and characterization of two novel thyroid hormone receptor beta isoforms.
584 *Mol Cell Biol.* 2000;20(22):8329-42. doi: 10.1128/mcb.20.22.8329-8342.2000. PubMed PMID: 11046130;
585 PubMed Central PMCID: PMCPMC102140.
- 586 27. Jansen MS, Cook GA, Song S, Park EA. Thyroid hormone regulates carnitine palmitoyltransferase
587 α gene expression through elements in the promoter and first intron. *J Biol Chem.*
588 2000;275(45):34989-97. doi: 10.1074/jbc.M001752200. PubMed PMID: 10956641.
- 589 28. Thakran S, Sharma P, Attia RR, Hori RT, Deng X, Elam MB, et al. Role of sirtuin 1 in the regulation
590 of hepatic gene expression by thyroid hormone. *J Biol Chem.* 2013;288(2):807-18. Epub 2012/12/03. doi:
591 10.1074/jbc.M112.437970. PubMed PMID: 23209300; PubMed Central PMCID: PMCPMC3543030.
- 592 29. McGarry JD, Brown NF. The mitochondrial carnitine palmitoyltransferase system. From concept to
593 molecular analysis. *Eur J Biochem.* 1997;244(1):1-14. doi: 10.1111/j.1432-1033.1997.00001.x. PubMed
594 PMID: 9063439.
- 595 30. Lee K, Kerner J, Hoppel CL. Mitochondrial carnitine palmitoyltransferase 1a (CPT1a) is part of an
596 outer membrane fatty acid transfer complex. *J Biol Chem.* 2011;286(29):25655-62. Epub 2011/05/26. doi:
597 10.1074/jbc.M111.228692. PubMed PMID: 21622568; PubMed Central PMCID: PMCPMC3138250.
- 598 31. Wu J, Wang C, Li S, Wang W, Li J, Chi Y, et al. Thyroid hormone-responsive SPOT 14 homolog
599 promotes hepatic lipogenesis, and its expression is regulated by liver X receptor α through a sterol
600 regulatory element-binding protein 1c-dependent mechanism in mice. *Hepatology.* 2013;58(2):617-28.
601 Epub 2013/07/02. doi: 10.1002/hep.26272. PubMed PMID: 23348573.
- 602 32. Anderson GW, Zhu Q, Metkowsky J, Stack MJ, Gopinath S, Mariash CN. The *Thrsp* null mouse
603 (*Thrsp(tm1cnm)*) and diet-induced obesity. *Mol Cell Endocrinol.* 2009;302(1):99-107. Epub 2009/01/20. doi:
604 10.1016/j.mce.2009.01.005. PubMed PMID: 19356628; PubMed Central PMCID: PMCPMC2671690.
- 605 33. Maia AL, Kieffer JD, Harney JW, Larsen PR. Effect of 3,5,3'-Triiodothyronine (T3) administration
606 on *dio1* gene expression and T3 metabolism in normal and type 1 deiodinase-deficient mice. *Endocrinology.*
607 1995;136(11):4842-9. doi: 10.1210/endo.136.11.7588215. PubMed PMID: 7588215.

- 608 34. Zavacki AM, Ying H, Christoffolete MA, Aerts G, So E, Harney JW, et al. Type 1 iodothyronine
609 deiodinase is a sensitive marker of peripheral thyroid status in the mouse. *Endocrinology*.
610 2005;146(3):1568-75. Epub 2004/12/09. doi: 10.1210/en.2004-1392. PubMed PMID: 15591136.
- 611 35. Goodridge AG, Adelman TG. Regulation of malic enzyme synthesis by insulin triiodothyronine, and
612 glucagon in liver cells in culture. *J Biol Chem*. 1976;251(10):3027-32. PubMed PMID: 944696.
- 613 36. Towle HC, Mariash CN, Oppenheimer JH. Changes in the hepatic levels of messenger ribonucleic
614 acid for malic enzyme during induction by thyroid hormone or diet. *Biochemistry*. 1980;19(3):579-85. doi:
615 10.1021/bi00544a029. PubMed PMID: 7356948.
- 616 37. Bianco AC, Salvatore D, Gereben B, Berry MJ, Larsen PR. Biochemistry, cellular and molecular
617 biology, and physiological roles of the iodothyronine selenodeiodinases. *Endocr Rev*. 2002;23(1):38-89.
618 doi: 10.1210/edrv.23.1.0455. PubMed PMID: 11844744.
- 619 38. Schneider MJ, Fiering SN, Thai B, Wu SY, St Germain E, Parlow AF, et al. Targeted disruption of
620 the type 1 selenodeiodinase gene (*Dio1*) results in marked changes in thyroid hormone economy in mice.
621 *Endocrinology*. 2006;147(1):580-9. Epub 2005/10/13. doi: 10.1210/en.2005-0739. PubMed PMID:
622 16223863.
- 623 39. Iritani N. Nutritional and hormonal regulation of lipogenic-enzyme gene expression in rat liver. *Eur*
624 *J Biochem*. 1992;205(2):433-42. doi: 10.1111/j.1432-1033.1992.tb16797.x. PubMed PMID: 1349281.
- 625 40. Shimomura I, Shimano H, Korn BS, Bashmakov Y, Horton JD. Nuclear sterol regulatory element-
626 binding proteins activate genes responsible for the entire program of unsaturated fatty acid biosynthesis in
627 transgenic mouse liver. *J Biol Chem*. 1998;273(52):35299-306. doi: 10.1074/jbc.273.52.35299. PubMed
628 PMID: 9857071.
- 629 41. Wagner RL, Huber BR, Shiau AK, Kelly A, Cunha Lima ST, Scanlan TS, et al. Hormone selectivity
630 in thyroid hormone receptors. *Mol Endocrinol*. 2001;15(3):398-410. doi: 10.1210/mend.15.3.0608. PubMed
631 PMID: 11222741.
- 632 42. Haning H, Woltering M, Mueller U, Schmidt G, Schmeck C, Voehringer V, et al. Novel heterocyclic
633 thyromimetics. *Bioorg Med Chem Lett*. 2005;15(7):1835-40. doi: 10.1016/j.bmcl.2005.02.028. PubMed
634 PMID: 15780617.

- 635 43. Erion MD, Cable EE, Ito BR, Jiang H, Fujitaki JM, Finn PD, et al. Targeting thyroid hormone
636 receptor-beta agonists to the liver reduces cholesterol and triglycerides and improves the therapeutic index.
637 Proc Natl Acad Sci U S A. 2007;104(39):15490-5. Epub 2007/09/18. doi: 10.1073/pnas.0702759104.
638 PubMed PMID: 17878314; PubMed Central PMCID: PMCPMC1978486.
- 639 44. Kirschberg TA, Jones CT, Xu Y, Fenaux M, Halcomb RL, Wang Y, et al. Selective Thyroid Hormone
640 Receptor β Agonists with Oxadiazolone Acid Isosteres. Bioorganic & Medicinal Chemistry Letters.
641 2020;127465. doi: <https://doi.org/10.1016/j.bmcl.2020.127465>.
- 642 45. Kalliokoski A, Niemi M. Impact of OATP transporters on pharmacokinetics. Br J Pharmacol.
643 2009;158(3):693-705. Epub 2009/09/25. doi: 10.1111/j.1476-5381.2009.00430.x. PubMed PMID:
644 19785645; PubMed Central PMCID: PMCPMC2765590.
- 645 46. Rodríguez-Antona C, Donato MT, Boobis A, Edwards RJ, Watts PS, Castell JV, et al. Cytochrome
646 P450 expression in human hepatocytes and hepatoma cell lines: molecular mechanisms that determine
647 lower expression in cultured cells. Xenobiotica. 2002;32(6):505-20. doi: 10.1080/00498250210128675.
648 PubMed PMID: 12160483.
- 649 47. Columbano A, Chiellini G, Kowalik MA. GC-1: A Thyromimetic With Multiple Therapeutic
650 Applications in Liver Disease. Gene Expr. 2017;17(4):265-75. Epub 2017/06/13. doi:
651 10.3727/105221617X14968563796227. PubMed PMID: 28635586; PubMed Central PMCID:
652 PMCPMC5885148.
- 653 48. Taub R, Chiang E, Chabot-Blanchet M, Kelly MJ, Reeves RA, Guertin MC, et al. Lipid lowering in
654 healthy volunteers treated with multiple doses of MGL-3196, a liver-targeted thyroid hormone receptor- β
655 agonist. Atherosclerosis. 2013;230(2):373-80. Epub 2013/08/21. doi:
656 10.1016/j.atherosclerosis.2013.07.056. PubMed PMID: 24075770.
- 657 49. Lian B, Hanley R, Schoenfeld S. A PHASE 1 RANDOMIZED, DOUBLE-BLIND, PLACEBO-
658 CONTROLLED, MULTIPLE ASCENDING DOSE STUDY TO EVALUATE SAFETY, TOLERABILITY AND
659 PHARMACOKINETICS OF THE LIVER-SELECTIVE TR-BETA AGONIST VK2809 (MB07811) IN
660 HYPERCHOLESTEROLEMIC SUBJECTS. Journal of the American College of Cardiology. 2016;67(13
661 Supplement):1932. doi: 10.1016/s0735-1097(16)31933-7.

662 50. Zhou J, Waskowicz LR, Lim A, Liao XH, Lian B, Masamune H, et al. A Liver-Specific Thyromimetic,
663 VK2809, Decreases Hepatosteatorsis in Glycogen Storage Disease Type Ia. *Thyroid*. 2019;29(8):1158-67.
664 doi: 10.1089/thy.2019.0007. PubMed PMID: 31337282; PubMed Central PMCID: PMC6707038.

665

666 Supporting information captions

667 **S1 Fig. THR agonist dose-response curves as calculated by RQ of THR targets in Huh-7 cells**

668 (A) *ANGPLT4*, (B) *CPT1A*, and (C) *DIO1* RNA levels were quantified in the same cells described in Fig 2C
669 and in the same manner. Results are presented as expression relative to the expression levels in control,
670 vehicle-treated cells. Representative mean RQ values at each compound concentration and fitted dose-
671 response curves are reported. (D) *ANGPLT4*, *CPT1A*, and *DIO1* RNA levels were quantified in the same
672 cells described in Fig 2C and in the same manner. Ct values of each gene for control, vehicle-treated groups
673 are reported. Results are presented as mean Ct values \pm SEM.

674 **S2 Fig. Modulation of serum lipid levels after single-dose treatment with MGL-3196 or T3 in HFD fed** 675 **rats**

676 (A) Total cholesterol measurements were obtained from serum of the same rats described in Fig 3D. Total
677 cholesterol level means \pm SEM are reported. Statistical analysis was performed using Brown-Forsythe and
678 Welch ANOVA tests and the mean of each group was compared to the mean of the HFD fed, vehicle-
679 control group; **P < 0.01, ***P < 0.001, ****P < 0.0001. (B) LDL-C measurements were obtained from serum
680 of the same rats described in Fig 3E. LDL-C level means \pm SEM are reported. Statistical analysis was
681 performed using Brown-Forsythe and Welch ANOVA tests and the mean of each group was compared to
682 the mean of the HFD fed, vehicle-control group; *P<0.05, **P < 0.01, ****P<0.0001. (C) Raw total
683 cholesterol levels reported in A) were used for calculations and are the same as those used for calculations
684 of data reported in Fig 3D. Results are presented as percent difference from the HFD fed, vehicle-control
685 group, post-dose. Percent change means \pm SEM are reported with mean values annotated within the bars.
686 Statistical analysis was performed using Brown-Forsythe and Welch ANOVA tests and the mean of each
687 group was compared to the mean of the HFD fed, vehicle-control group; **P<0.01,***P<0.001, ****P <
688 0.0001. (D) LDL-C levels reported in B) were used for calculations and are the same as those used for
689 calculations of data reported in Fig 3E. Results are presented as percent difference from the HFD fed,
690 vehicle-control group, post-dose. Percent change means \pm SEM are reported with mean values annotated
691 within the bars. Statistical analysis was performed using Brown-Forsythe and Welch ANOVA tests and the

692 mean of each group was compared to the mean of the HFD fed, vehicle-control group; *P < 0.05, **P <
693 0.01, ****P < 0.0001.

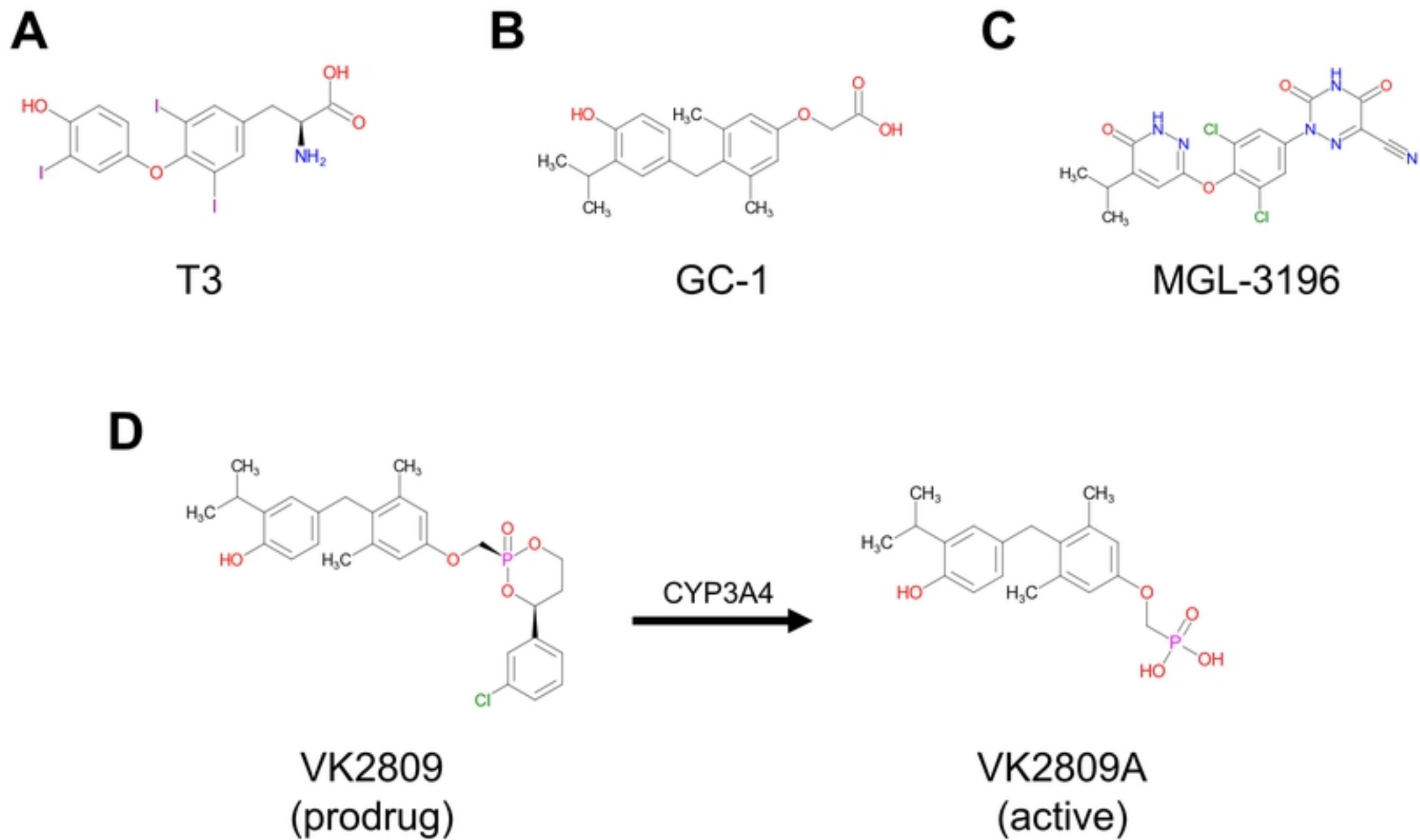


Figure 1

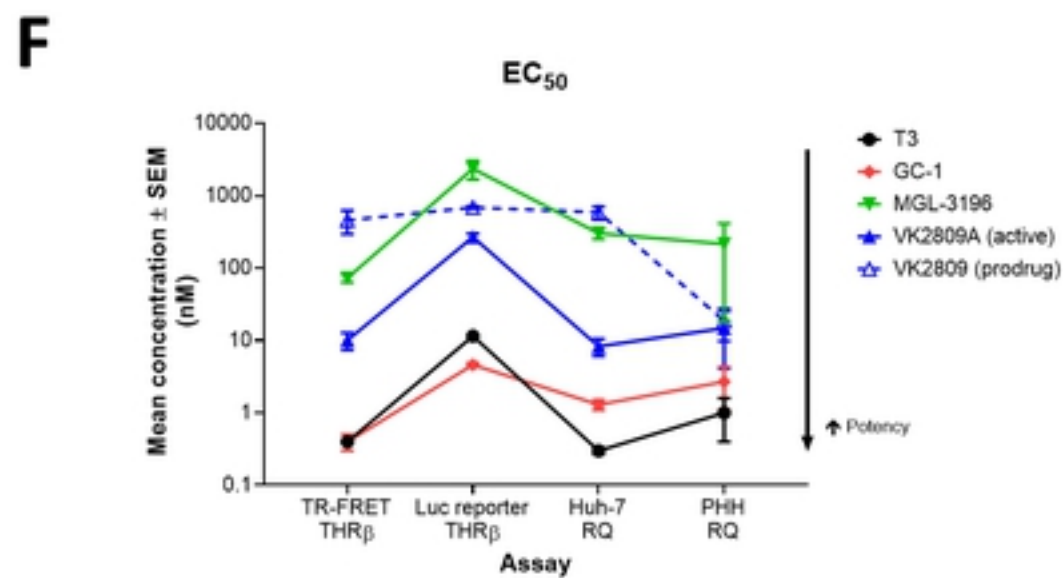
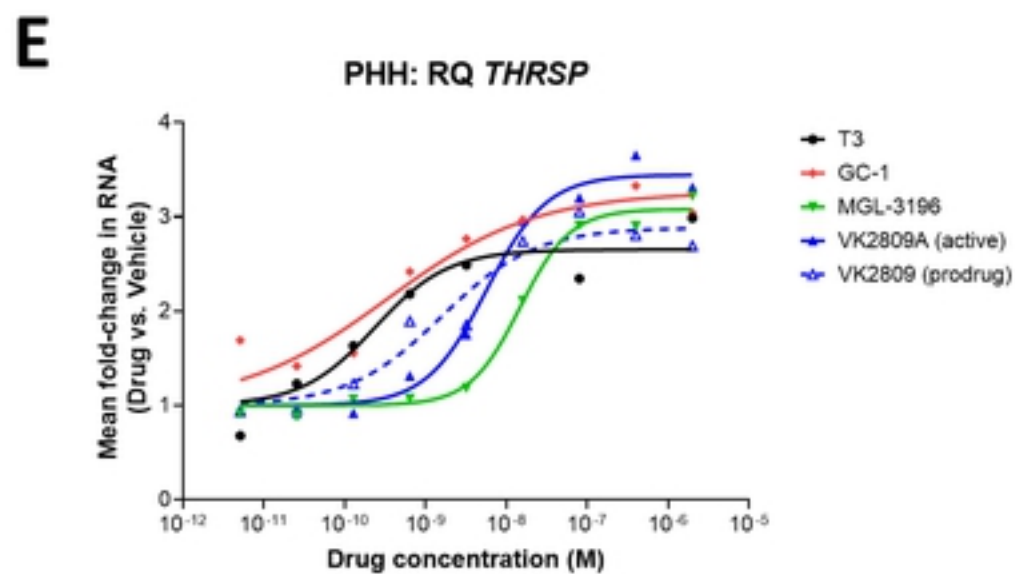
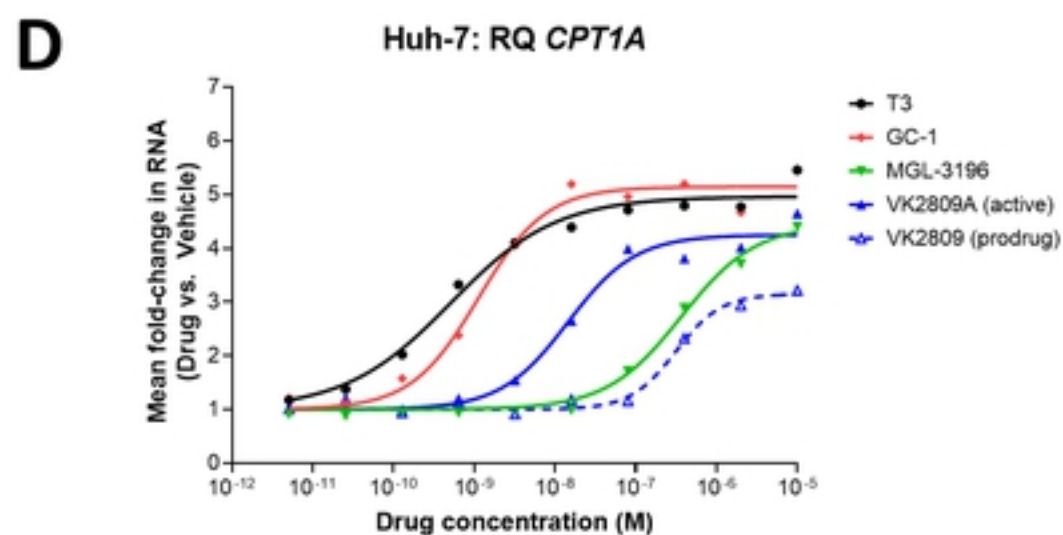
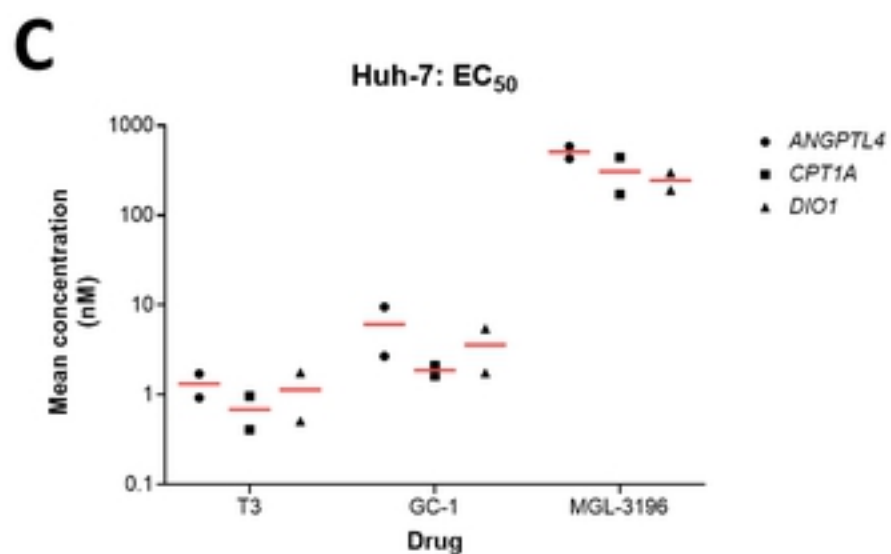
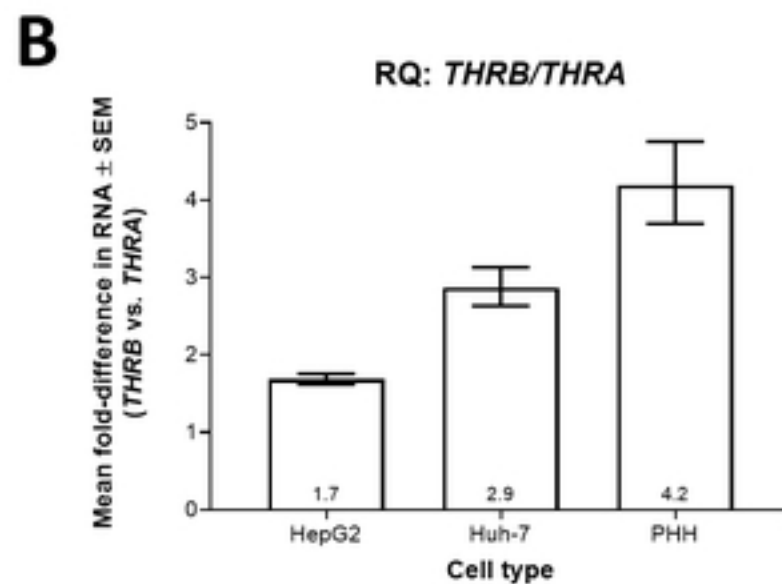
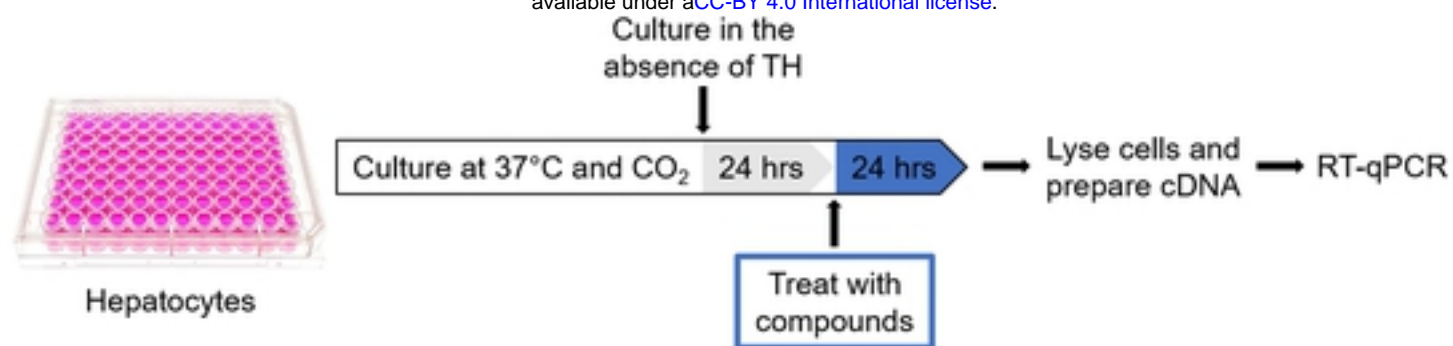
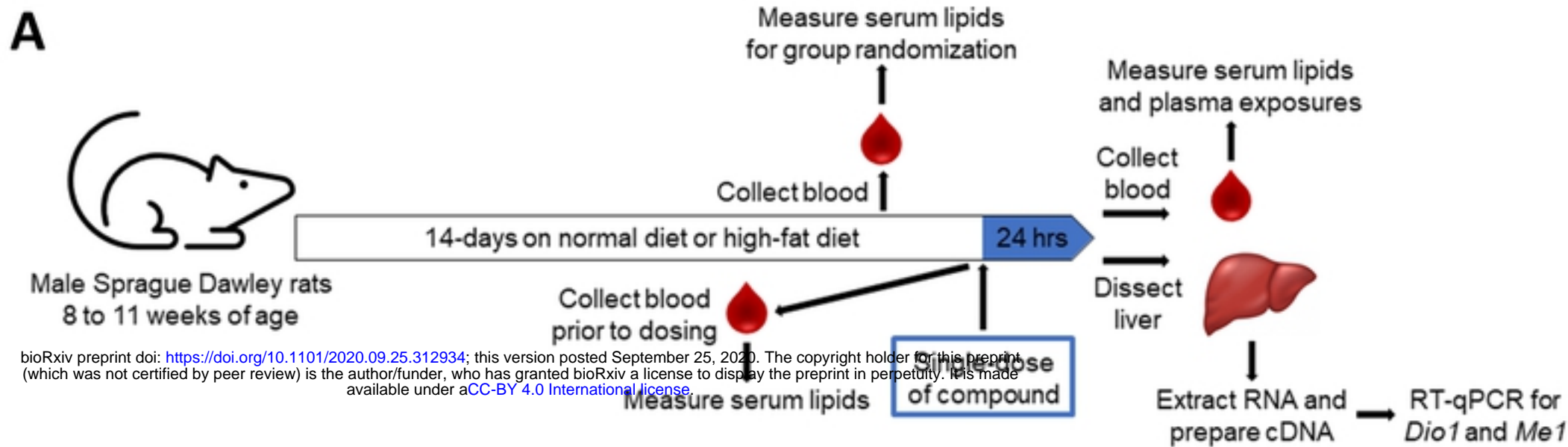


Figure2



bioRxiv preprint doi: <https://doi.org/10.1101/2020.09.25.312934>; this version posted September 25, 2020. The copyright holder for this preprint (which was not certified by peer review) is the author/funder, who has granted bioRxiv a license to display the preprint in perpetuity. It is made available under aCC-BY 4.0 International license.

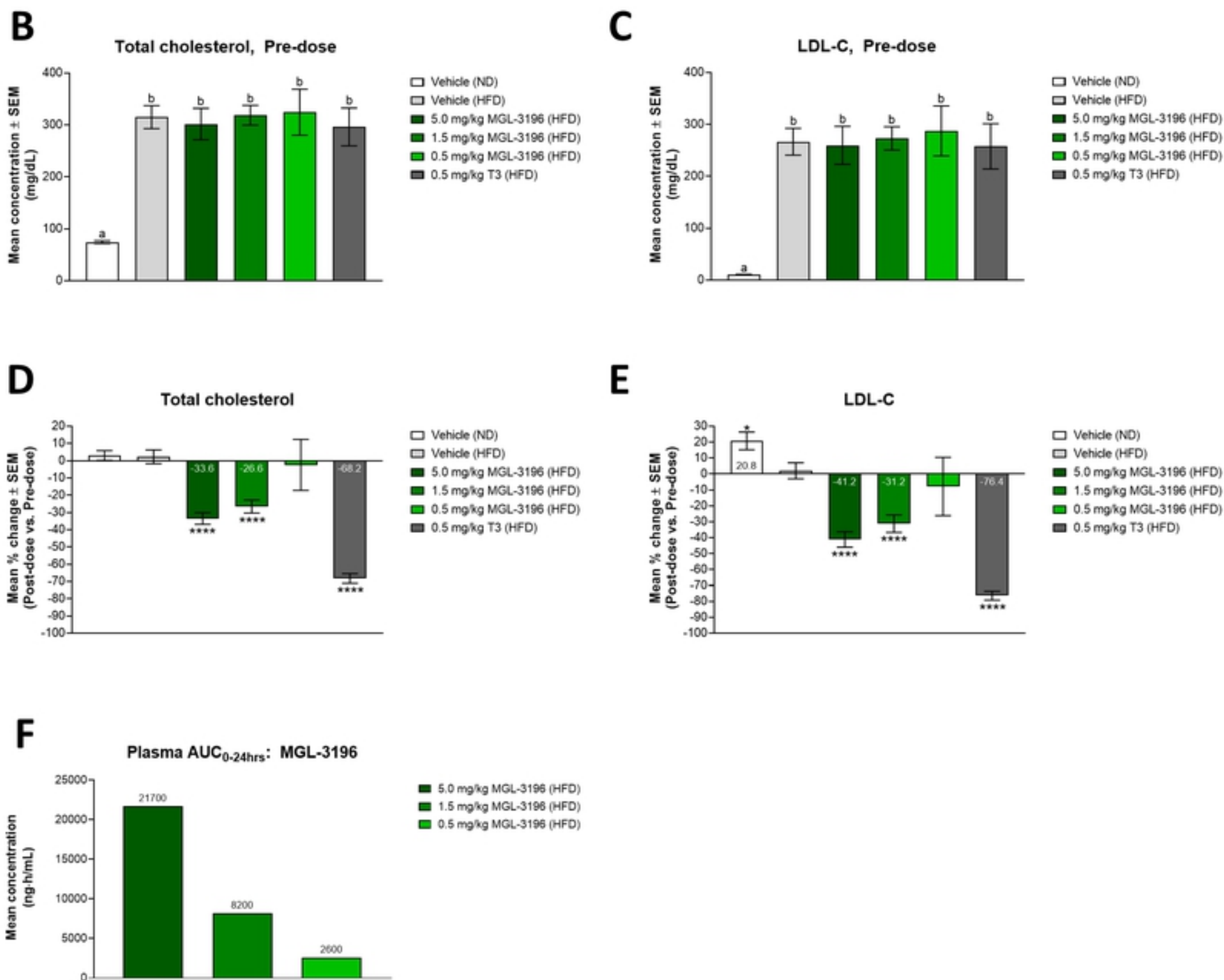
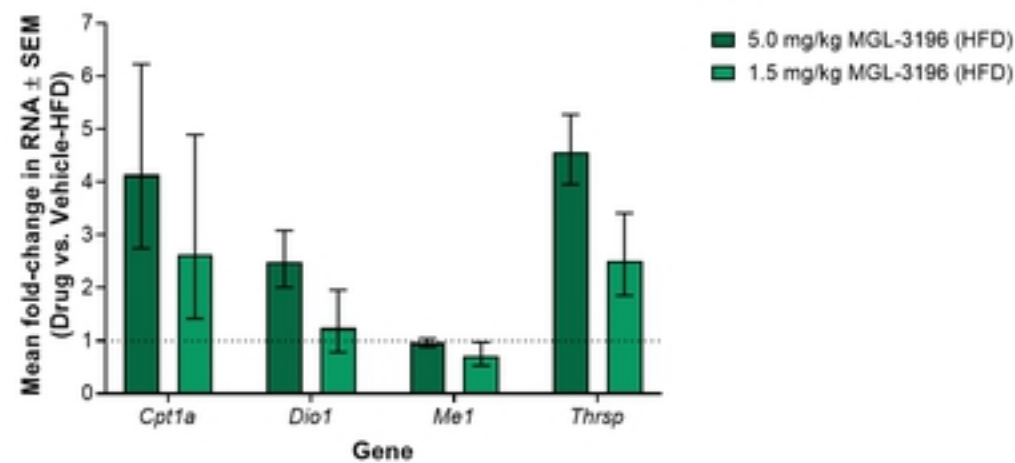


Figure3

A

RQ: 4 hrs post-dose

**B**

RQ: 24 hrs post-dose

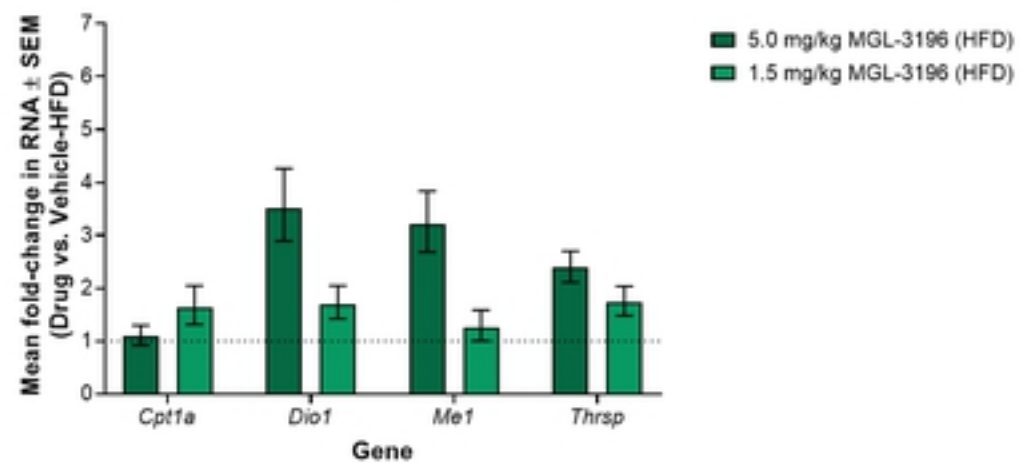
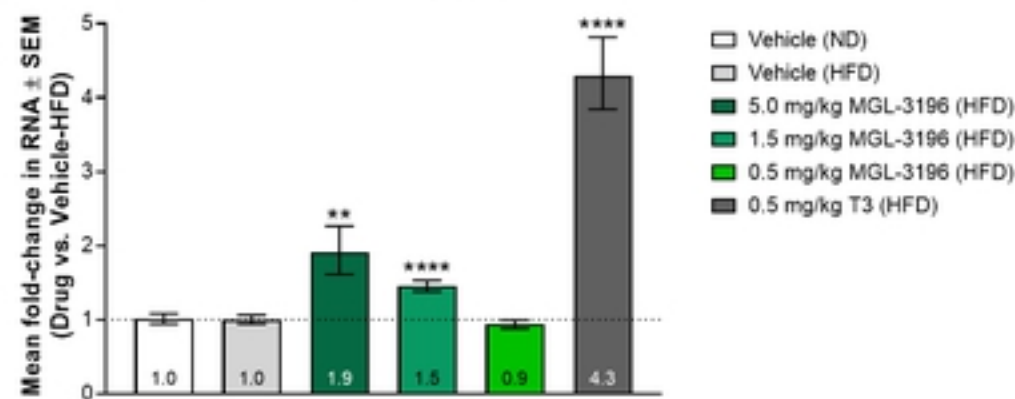
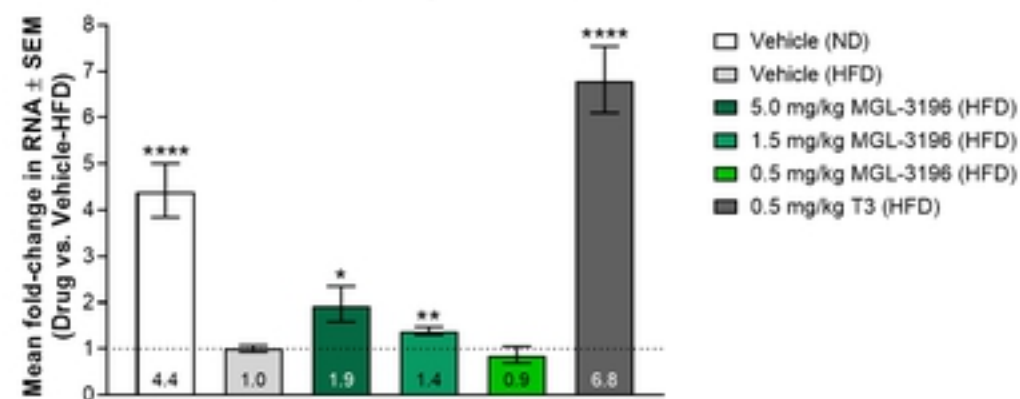
**C**RQ *Dio1*: 24 hrs post-dose**D**RQ *Me1*: 24 hrs post-dose

Figure 4